2-17-2011

# SBS-based Radar True Time Delay

Mark Bashkansky
*Naval Research Laboratory*

David Walker
*Naval Research Laboratory*

Armen Gulian
*Chapman University*, gulian@chapman.edu

Michael Steiner
*Naval Research Laboratory*

## Recommended Citation

Bashkansky M., Walker D., Gulian A. and Steiner M., SBS-based Radar True Time Delay. Advances in slow and fast light IV (Eds.: Shahriar, S.M. and Hemmer, P.R.): *Proceedings of SPIE*, vol. **7949**, 2011, Article # 794918. https://doi.org/10.1117/12.880792

# SBS-based Radar True Time Delay

## Comments

## Copyright

# SBS-based Radar True Time Delay

Mark Bashkansky*, David Walker, Armen Gulian, Michael Steiner

Naval Research Laboratory, Washington DC, USA 20375-5320

## ABSTRACT

Stimulated Brillouin scattering (SBS) based slow light is considered for application to squint-free (true time delay) steering of phased array radar antennae. Results are presented on true time delay radar requirements, including delay precision and bandwidth. We experimentally investigated the level of delay precision that exists in actual slow-light systems (based on Brillouin scattering). The practical use of SBS to meet the necessary requirements for radar use is discussed.

**Keywords:** Antenna arrays, radar, slow light, optical fibers, stimulated Brillouin scattering, Faraday rotator

## 1. INTRODUCTION

Phased array radars transmit and receive microwave radiation through an array of antenna elements. By phase shifting each element by a different and precise amount, a narrow beam is coherently steered in a particular direction without the need for mechanical scanning of the antenna. However, phased arrays run into a fundamental limit in regards to the range resolution. The range resolution of a sensor utilizing pulses of a particular bandwidth $B$ is $R = c/(2B)$, where $c$ is the speed of light in vacuum. This limit comes about from an effect known as "squinting", which is analogous to chromatic aberration and arises whenever high bandwidth signals are used.

Prior techniques to achieve an optical delay have been proposed based on both electronic microwave and optical delays; for example an optical delay is presented in [1]. In 1999 it was shown that significant reduction in the propagation speed of light was demonstrated with cold atoms [2]. Later stimulated Brillouin scattering (SBS) was shown to have slow-light features in common with the earlier 1999 work [3,4]. A major advantage of using SBS in optical fibers over cold atoms is the simplicity of the implementation and availability of off-the-shelf components. Slow light based on SBS also produces pure delays in a way that allows fast switching of the delay time. The authors undertook a study to determine the applicability of SBS to radar true time delay.

In previous papers the use of SBS has been investigated theoretically [5,6] for applicability to radar true time delay. In [5] we determined the effect of bandwidth on a purely phase steering radar. In [6] we quantified the delay precision needed to achieve a given level of performance. Additionally it was experimentally found that birefringence in optical fibers induces polarization changes which destabilize the SBS delay. A technique was demonstrated [7] in which reflection from a Faraday rotator mirror is used to cancel the effect of polarization changes on the slow light delay. In this paper we experimentally determine the level of delay precision that exists in actual Brillouin scattering. This is done in several ways and the techniques are largely found to be in agreement.

In Sec. 2 background is presented on the effects of bandwidth as well as stability requirements. In Sec. 3 wideband delay results are presented. The implications of these measurements on the use of SBS for TTD radar is discussed in Sec. 4.

*mark.bashkansky@nrl.navy.mil; phone 202-767-2512

# 2. BACKGROUND

In order to increase the range resolution of a radar, the bandwidth generally must be increased. The optimal technique for beam steering requires the entire signal to be delayed across the phased array elements to compensate for the time-delay of the incoming signal. However, nearly all modern phased arrays utilize phased array steering, which although a valid approximation for narrowband signals, results in degradation of the beam. For a specific example of squinting, consider a one-dimensional array of antennae at positions $x_j$, then the appropriate phase shifts to steer a beam into direction $\theta_0$ where $\varphi_0^{(j)} = \omega_0 x_j \sin(\theta_0)/c$ $\theta_0$ where $\omega_0$ is the (central) RF carrier frequency. Carrier frequencies often used in practice are S-band: $\omega_0/2\pi \sim 3$ GHz, and X-band: $\omega_0/2\pi \sim 10$ GHz. For sufficiently large signal bandwidth $B$, applying phase shifts $\varphi_0^{(j)}$ leads to squinting. In [6] an analysis was performed to determine the requirements for TTD radar. These results are briefly reproduced here for convenience.

TTD eliminates the squinting by providing phase shifts that vary linearly with frequency. In particular, the array factor as defined in [6] becomes

$$A^{(TTD)}(\theta, \omega) = \sum_j a_j \exp[i\omega(u - u_0)x_j / c] \tag{1}$$

The actual signal frequency $\omega$ (rather than the center frequency $\omega_0$) determines the steering phase shift applied $\varphi^{(j)}(\omega) = \omega u_0 x_j/c$. The physical delay applied to achieve this is $\tau_d^{(j)} = \varphi^{(j)}(\omega)/\omega = u_0 x_j/c$. Calculation of the array factor (1) reveals that the perfect beam forming is recovered even for large bandwidths $B$. The solid curve in Fig. 1(a) is an example for $N$=128 elements, X-band, with B=1 GHz. In a TTD system, a large $B$ can reduce the sidelobe variations, but leaves the mainlobe intact.

In order to scan the beam, one must be able to adjust the delays at each element over the required range. Note that only the *relative* delay affects the beam steering, so one would design the system so the element at one end ($j$=1) would not need any delay adjustment, while the far end element ($j = N$) would have the maximum required adjustable delay range $\tau_d^{(max)} = u_0 L/c$, where $L = N \lambda_0 / 2$ is the total size of the array. In the extreme limit of 90 degree steering, $u_0 = 1$ and $\tau_d^{(max)}$ is simply the time for light to propagate a distance $L$. For an X-band system with $N = 128$ elements, and 60 degree steering, $\tau_d^{(max)} = 5.5$ ns, while an S-band system with the same number of elements, due to the larger $\lambda_0$, would require $\tau_d^{(max)} = 18.3$ ns.

## 2.1 DELAY PRECISION

Unintended fluctuations of the individual element delays will degrade the coherent summation needed for beam forming and so one must be able to precisely control them. The dashed and dotted curves in Fig. 1(a) plot array factors where each element is given a random error in delay, with a Gaussian distribution of width $\tau^{(e)}$. One sees a degradation of the main lobe level (MLL). It also elevates the side lobe level and introduces some random fluctuations in the sidelobes, which is an important consideration when performing clutter suppression. Fig. 1(b) plots the MLL loss as a function of $\tau^{(e)}$ for $N$=128. We confirmed that this loss was independent of $N$ in all cases and that 1 dB of loss occurs at $\tau^{(e\text{-crit})} = 8$ ps. This time-scale is related to the time for light propagation across one element which is $\lambda_0/2c = 1/2f = 50$ ps (though the exact value of $\tau^{(e\text{-crit})}$ tolerance depends on our choice of the critical loss, chosen to be 1 dB in this analysis). Note, however, that the *relative* delay control required does depend on $N$. For example, for $N = 128$, $\tau^{(e\text{-crit})}/\tau_d^{(max)} = 0.0015$ (or 28 dB dynamic range) and every factor of two in $N$ will add 3 dB of dynamic range requirement. An S-band radar, would have $\tau^{(e\text{-crit})} = 27$ ps (though a correspondingly larger delay range, so the dynamic range requirement would be the same).

Note from the beam patterns in Fig. 1(a) that the sidelobe level rises dramatically with delay fluctuations. Fig. 1(c) shows the sidelobe level as a function of the time fluctuation level $\tau^{(e)}$. In particular, at $\tau^{(e\text{-crit})} = 8$ ps, the sidelobe level has gone from the designed (Taylor weighted) level of -40 dB to approximately -21 dB.

## 2.2 AMPLITUDE PRECISION

The other important characteristic is the precision with which the amplitude is preserved by the TTD process. Fig. 2(a) compares the array factor obtained with a perfect TTD and one with relative amplitude errors of $a^{(e)} = 0.2$. For this calculation, each amplitude $a_j$ is multiplied by a factor $(1+\alpha)$, where $\alpha$ is chosen from a Gaussian distribution of width $a^{(e)}$. We see that the amplitude errors have no effect on the main lobe, as the elements are all still perfectly phased and have symmetric positive and negative amplitude errors. However, the amplitude errors clearly inhibit the side lobe

suppression being performed by the Taylor weighting. Fig. 2(b) plots the largest side-lobe level versus $a^{(e)}$. We lose about 3 dB of suppression for $a^{(e)}$=0.05 (or 13 dB dynamic range). This is a remarkably weak sensitivity compared to the much more stringent delay precision requirements. In addition to amplitude fluctuations, one can also have random phase fluctuations. However, these are mathematically equivalent to the delay fluctuations using the corresponding phase error $\varphi^{(e)} = \omega_0 \tau^{(e)}$. Using this we find the critical phase error level for 1 dB loss is $\varphi^{(e)}$ =0.08.
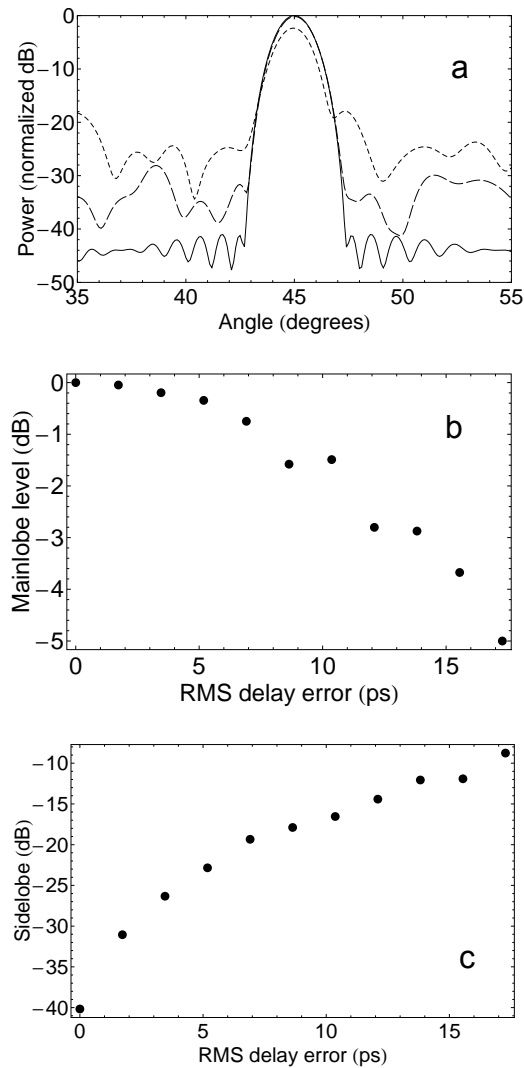


Fig. 1: Effect of delay precision in beam forming. $\omega$= $(2\pi)$ 10 GHz center frequency with B=$(2\pi)$ 1 GHz bandwidth. (a) Array factor $A_B^{(TTD)}(\theta)$ of an $N$=128 element array with perfect TTD (solid curve) and array factors with RMS fluctuations in the delays of $\tau^{(e)}$=3 ps (dashed) and $\tau^{(e)}$=11 ps (dotted) (b) MLL loss at $\theta_0$=30 degrees versus delay fluctuation $\tau^{(e)}$. (c) Side lobe level (SLL) at $\theta_0$=30 degrees versus delay fluctuation $\tau^{(e)}$.
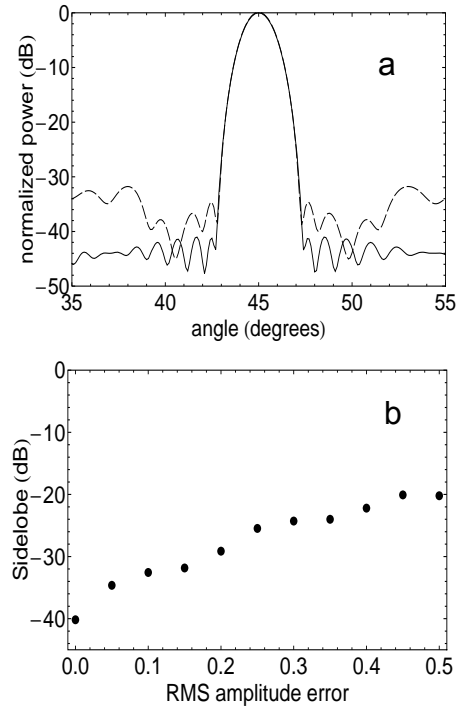
Fig. 2. Effect of amplitude fluctuations in beam forming. $\omega = (2\pi)$ 10 GHz center frequency with $B=(2\pi)$ 1 GHz bandwidth. (a) Array factor of an $N$=128 element array, steering at $\theta_0$=30 degrees, with perfect TTD (solid curve) and with amplitude fluctuations $a^{(e)}$ =0.2 (dashed). (b) Maximum SLL versus amplitude fluctuation $a^{(e)}$.

## 3. DELAY FLUCTUATIONS

In this Section, SBS measurements are presented. Optical delay prototypes for single and multiple channel systems were built and tested. Other issues with multiple elements are discussed at the end of Sec. 3.

A simplified schematic of the single-element characterization setup is shown below in Fig. 3. (A closer representation of the experimental setup is shown in Fig. 7 (and described in the accompanying text), which differs only in having many input lasers multiplexed together and corresponding demultiplexing at the output.) Light from a laser diode provides the pump beam, which is amplified by the erbium doped fiber amplifier (EDFA). A polarization-maintaining voltage-controlled optical attenuator (VOA) [not shown] is used to adjust the pump power, so that the EDFA settings can be set to a constant optical output power of 250mW. The pump then passes through the polarization-maintaining circulator and reaches the polarizing beam combiner. A second laser provides the Stokes beam. A Mach–Zehnder electro-optic modulator creates a pulse envelope for the Stokes beam which then passes through another polarization-maintaining circulator. A small length of fiber rotates the Stokes beam polarization by 90 degrees, to allow Stokes and pump to be combined at the polarizing beam combiner. Both lasers run CW at a wavelength near 1548 nm. The Stokes laser is tuned to be 9.66 GHz below the pump laser frequency, as this is the Brillouin frequency for our spool of optical fiber. At the polarizing beam combiner, the pump beam and Stokes beam have $p$ and $s$ polarizations, respectively. Once combined the pump and Stokes co-propagate through the special small-core optical fiber spool (of length 1.5 km), encounter a Faraday rotator mirror which rotates their polarizations by 90 degrees and reflects them back. Both of the pairs of counter propagating Stokes and pump contribute to the Stokes gain. The retro-reflected Stokes beam emerges from the third port of the circulator in the pump branch, where it is measured by a photodiode. From the laser diode up to the polarizing beam combiner, all the optical fibers in our setup are polarization maintaining.

While previously, we have used a single laser to produce the Stokes and pump beams (splitting power from a single laser diode into two arms, one of which is modulated with an EOM to create a sideband shifted by the Brillouin frequency of our gain medium), here we use two separate lasers, tuned to the appropriate frequency difference.
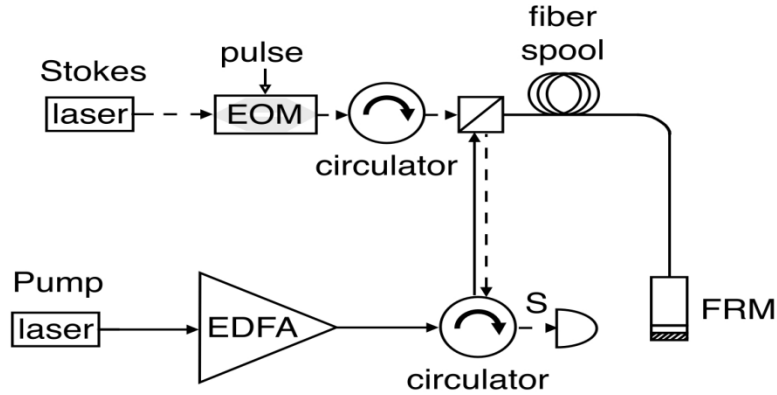
Fig. 3. SBS setup for slow light measurements. Two lasers provide pump and Stokes light. The electro-optic modulator (EOM) is used to transform the Stokes beam into a square wave pulse train consisting of 2 ns-long pulses. The erbium-doped fiber amplifier (EDFA) amplifies the pump beam to 250 mW. A polarization-maintaining voltage-controlled optical attenuator (VOA) [not shown] is used to vary the beam power. The pump and Stokes are combined at a polarizing beam splitter. They pass through the 1.5km of small-core fiber, reflect from the Faraday rotator mirror (FRM) , and propagate back through the small-core fiber.

In Fig. 4 we show Stokes amplification out versus pump power for the wideband case. Note that the amplified Stokes output power is approximately linear with the pump power. This is in sharp contrast to the narrowband case whereby it is the case that the gain is exponential with the pump power, see for example [7]. The reason for this is that there is generally a reduction in peak gain by a factor of $f = \left(1 + \frac{\Delta\omega_p}{\Gamma_B}\right)$ [8] where $\Delta\omega_p$ is the pump field spectral linewidth and $\Gamma_B$ is the SBS resonance linewidth. For the fiber used in this experiment, $\Gamma_B = 20$ MHz and $\Delta\omega_p = 1.8$ GHz. In this case f = 91. Because of this reduction in gain, Stokes out which is exponential in gain for the narrowband case, will be approximately linear since $\exp(I_0gL)$ is approximately linear in $I_0$ when $I_0gL \ll 1$. In fact for the narrowband case gL was estimated from the data $gL=.28$ and for the wideband case .28/91=.0031, and for the pump powers used it is seen that $I_0gL \ll 1$.
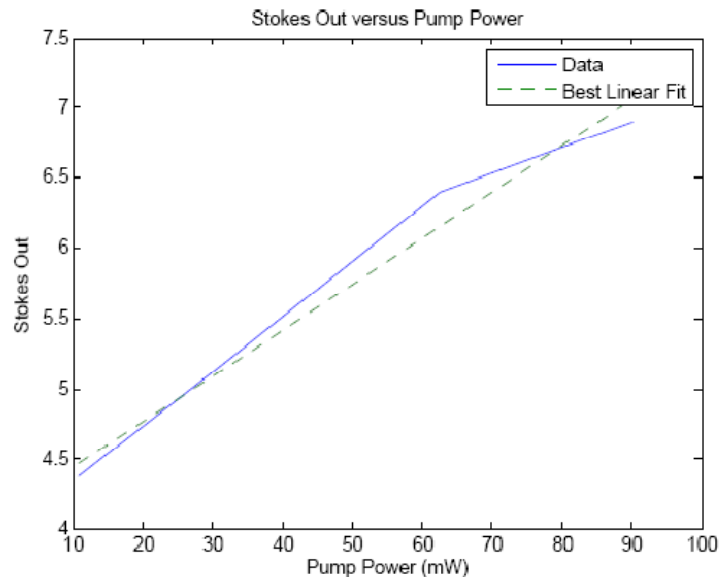


Fig. 4: Stokes out versus pump power. The dashed line represents a best linear fit.

In Fig. 5 relative delay is plotted versus pump power for the wideband case. It is seen that relative delays increase linearly with pump power as expected. The delays are significantly less than in the narrowband case. In [7] for example delays for the narrowband case with similar pump powers were found in the range of 0 to 50 ns. This is because the slope of the curve delay versus pump power is also affected by the factor f, so that the slope decreases in this case by 91. In order to maintain similar delays substantially more pump power would be necessary, which results in other problems. However, for X-Band, 200 ps is a reasonable delay to study.

While characterizing the delay precision or jitter, we found that direct measurement using our sampling oscilloscope was not sufficiently accurate since the oscilloscope had intrinsic jitter. In order to determine the time jitter we measured the Stokes amplitude fluctuations. From Fig. 4 the corresponding pump power fluctuations can be determined. A best linear fit was used to model the nearly linear dependence as seen in Fig. 4. Based on the slope of the line and the Stokes amplitude fluctuations, the pump fluctuations were found. The pump fluctuations were then used to determine the delay fluctuations from Fig. 5. Again, a best linear fit line is shown by the dashed lines in Fig. 5 whose slope was used to convert from pump fluctuations to delay fluctuations. Finally in Fig. 6 delay jitter versus pump power was found. This assumes that the major cause of time fluctuations is pump power fluctuations. Further investigation is needed to determine precisely what is causing the time jitter.
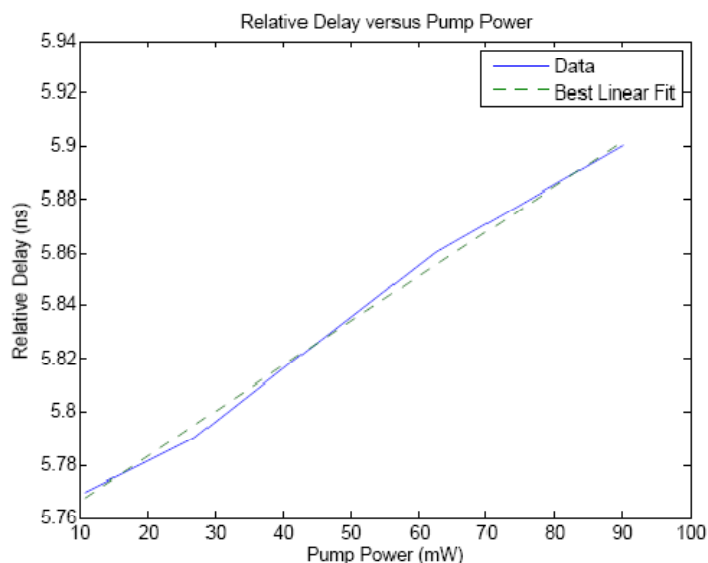


Fig. 5: Relative Delay versus Pump Power.  Dashed line is best linear fit
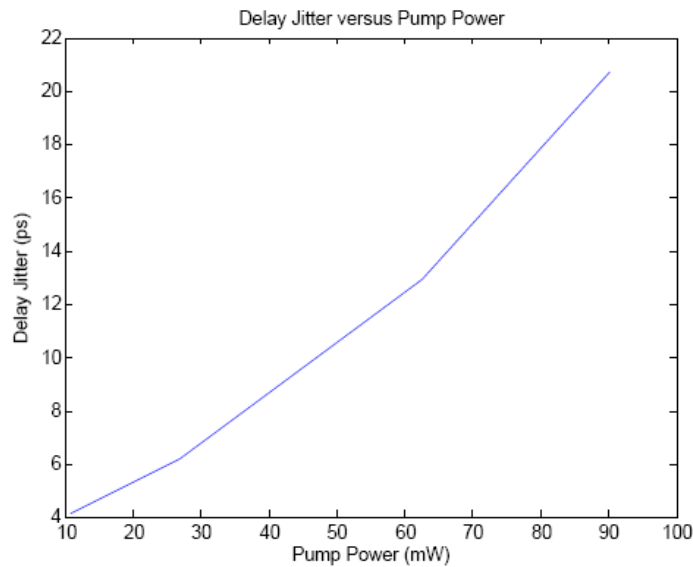
Fig. 6: Delay Jitter versus Pump Power

Figure 7 shows an approximation of the experimental setup for the multiple-channel SBS measurements. Again, this is essentially the same as the setup in Figure 3, except that several lasers are multiplexed together for both the Stokes and pump inputs, and the corresponding Stokes output is demultiplexed via a fiber-connected athermal grating. The multiplexing of inputs is achieved simply (but with a lot of loss) by combining beams together through binary trees of polarization-maintaining 50/50 couplers. Separate polarization-maintaining VOAs for each of the Stokes and pump channels are used to adjust the optical powers. In particular, these VOAs are important in getting the ratio of the pump lasers to be 1:2:3, so as to allow a simple scaling of the overall pump transmission to cause steering of the resulting radar beam. In this setup, the spacing between the optical setup was 100 GHz.

Figure 7 is an idealized version of the experimental setup. In the actual implementation, Stokes channel 0 (which required no corresponding pump channel as we did not delay it, using it instead as a reference) was not actually multiplexed into the small core fiber with the other channels. Rather, it propagated through a separate standard optical fiber. To compensate for the fact that its path was different, a separately timed pulse generator was used, such that the Stokes channel 0 pulse would reach its photodetector at the same time that the other (undelayed) pulses would reach their corresponding detectors, in the absence of pump power.

Also, to reduce the number of necessary lasers, power from one of the Stokes lasers was split into two paths to create an additional Stokes beam. As this second beam was for channel 0 and propagated in a separate fiber, the degeneracy of these two frequencies did not create any problems.

The purpose of the multi-channel setup was to determine if there would be any additional significant impediments to extending the single element predictions to multiple elements. Our approach to implementing multiple channels through multiplexing all optical frequencies into the same small-core optical fiber had one drawback: There appears to be additional PIEnoise when more than one channel is active. This additional noise may have contributions from a) crosstalk between the channels in the grating used for demultiplexing and b) a nonlinear mixing between the optical frequencies, due to processes other than Brillouin scattering. It may be possible to suppress these effects, and it would certainly be possible to implement a multi-channel system by giving each channel its own optical fiber.
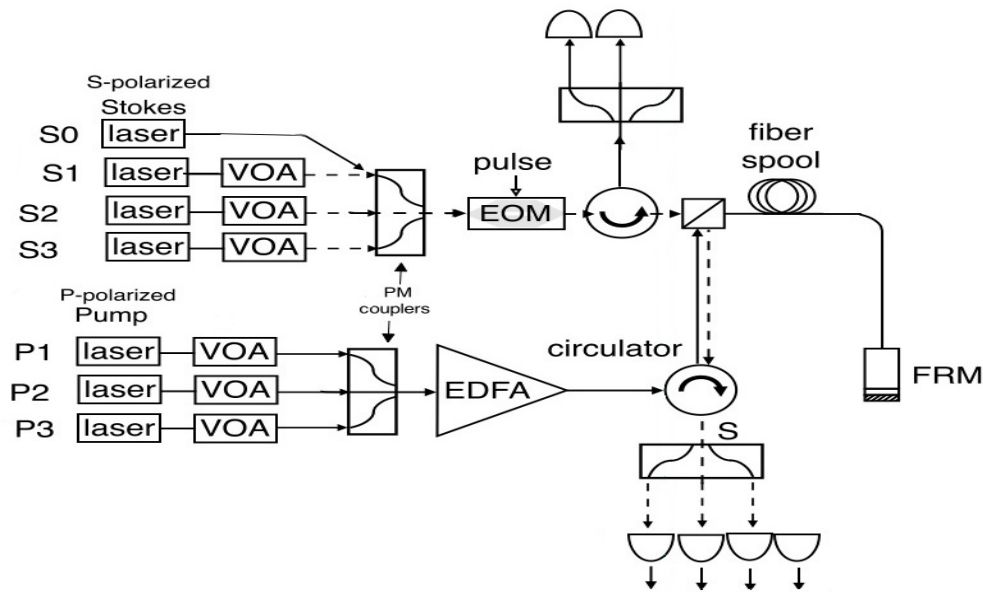
Fig. 7: Multiple channel version of the experimental setup for SBS-based slow light. Multiplexing is achieved by combining channels via polarization-maintaining couplers. Demultiplexing of the Stokes beam is performed with an athermal grating.

## 4. CONCLUSIONS

In conclusion, we investigated the limitations of using SBS as a true time delay element. We showed from simulations the degradation of the antenna pattern sidelobes in terms of the RMS jitter. Additionally we characterized the jitter seen in SBS. A reasonable baseline could be considered from these results whereby one desired a 1 GHz bandwidth at X-Band with 30 dB sidelobes and minimal sidelobe degradation. One can see from Fig. 1c that the requirement would be 5 ps jitter. On the other hand, we see that the jitter from Fig. 6 is greater than 5 ps for all but small pump powers. This significant level of noise that we found in SBS was admittedly unexpected, but appeared to be prevalent. Investigation of the sources of the additional noise is a subject for future research. Because of this, in order for SBS to meet the requirements for high frequency radars such as X-Band, additional steps would need to be taken to reduce the level of noise. For example, it is possible that the system could be further stabilized to reduce amplitude fluctuations in the pump laser. On the other hand we expect that SBS as a true time delay element could be used to meet requirements at lower frequencies such as S-Band. However, currently the complexity of implementation is still significant compared with other alternative techniques such as [1]. Additionally we built and tested a multiple element system. It was found that additional noise is introduced in a multiple element system, although we did not see any significant impediments in achieving the expected multiple element performance from that predicted via the single element characterization.

## ACKNOWLEDGMENTS

## REFERENCES

[1] Frigyes, I. "Optically generated true-time delay in phased-array radars," IEEE Trans. Microwave Theory and Techniques, 43, 2378-2386 (1995).
[2] Hau, L. V., Harris, S. E., Dutton, Z., and Behroozi, C. H., "Light speed reduction to 17 metres per second in an ultracold atomic gas," Nature, 397, 594-598 (1999).

[3] Zhu, Z. and Gauthier, D. J., "Nearly transparent SBS slow light in an optical fiber," Opt. Express, 14, 7238-7245 (2006).

[4] Boyd, R. W., Gauthier, D. J., Gaeta, A. L., and Willner, A. E., "Maximum time delay achievable on propagation through a slow-light medium," Phys. Rev. A, 71, 023801 (2005).

[5] Dutton, Z., Gulian, A., Bashkansky, M., and Steiner, M., [Slow Light: Science and Applications], CRC Press, (2008).

[6] Bashkansky, M., Dutton, Z., Gulian, A., Walker, D., Fatemi, F., and Steiner, M., "True-Time Delay Steering of Phased Array Radars Using Slow Light", Proceedings of SPIE, 7226, 72260A-1 (2009)

[7] Walker, D. R., Bashkansky, M., Gulian, A., Fatemi, F. K., and Steiner, M. "Stabilizing slow light delay in stimulated Brillouin scattering using a Faraday rotator mirror," J. Opt. Soc. Am. B, 25, C61-C64 (2008).

[8] Dawes, A. M., Zhu, Z., Gauthier, D. J., "Improving the bandwidth of SBS-based slow-light delay," Conference on Lasers and Electro-Optics and Quantum Electronics, (2006).